TRANSFUSION OF TIME-DOMAIN AND FREQUENCY-DOMAIN EDDY CURRENT SIGNALS

Ibrahim Elshafiey, Majeed Alkanhal, and Ayed Algarni

Electrical Engineering Department, King Saud University, P.O. Box 800, Riyadh 1142, Saudi Arabia
e-mail: ishafiey@ksu.edu.sa

ABSTRACT

Conventional eddy current using single-frequency excitation has limited material characterization capabilities. Enrichment of the spectral information of the signal with techniques such as multifrequency or swept frequency inspection could be employed to improve the inspection process. Broadband excitation is also implemented with time-domain inspection using pulsed eddy current PEC. The spectrum of PEC however has decayed energy corresponding to higher frequencies.

This paper addresses the implementation of a technique, termed transfusion; to fuse partial eddy current information obtained from measurements in the time domain with PEC with inspection results that could be available at fixed points in the frequency domain, obtained with conventional eddy current inspection. The technique is based on image fusion methods, in accordance with increased interest in c-scan representation of eddy current signals. The developed algorithm depends on packing multi-spectral and multi-temporal data into the values of color components of transfusion image. Further enhancement could be obtained by fusing this image with a high quality image of the object under test, which could be acquired using high frequency eddy current inspection or another NDE modality. Results based on the proposed technique, based on finite element simulation of eddy current inspection are presented, along with suggested image quality measures to test the spectral as well as spatial information of the transfusion image.

Keywords: NDE, Pulsed Eddy Current, Wavelet Analysis, Image Fusion.

1. INTRODUCTION

Eddy current (EC) techniques are widely used to inspection conductive materials such as aircraft skin. Conventional eddy current depend on harmonic analysis in which

sinusoidal excitation is used. Due to the skin effect, high frequency excitation with low penetration depth is used for detecting surface features, while low frequency values are used to inspect subsurface features. Single-frequency excitation has thus limited material characterization capabilities and data that are more rigorous could be obtained by enhancing the spectral information with techniques such as multifrequency or swept frequency inspection.

Broadband excitation is also implemented with time-domain inspection using pulsed eddy current (PEC) methodology developed to improve the efficiency of eddy current testing in detecting corrosion and deep flaws. In PEC, an electric pulse is applied to a driving coil. The secondary magnetic field is recorded using an inductive coil or magnetic sensor. Application example is in inspecting fuselage lap joint multi-layer structure where fatigue cracks are not necessarily confined to the upper layer. Corrosion of the lap splice tends to alter the stress state and shift the maximum stress to second or third skin layers skin [Giguere1, 02].

Various techniques have been developed to cast eddy current signals obtained using harmonic as well as pulsed eddy current inspection data in the form of C-scan images [Udpa, 01]. Images provide natural way of analyzing the eddy current signal. PEC provides also a powerful tool to obtain information related to various depths in material. Observation time interval and a sampling rate can be used for "in-depth slicing" of conductive media [Plotnikiv, 07] and [Plotnikiv, 02].

This paper provides a tool to fuse partial eddy current information obtained from measurements in both time domain (using PEC) and particular frequency domains nodes (with harmonic analysis). The technique is based on image fusion methods.

2. TIME-DOMAIN AND FREQUENCY-DOMAIN EDDY CURRENT SIGNALS

Harmonic eddy current signal provide information about certain point in the spectrum, where time domain representation is simple sinusoidal form. Information is obtained as complex phasor representing probe impedance. C-scan images could be obtained to reflect map of real part, imaginary part, or the magnitude of probe impedance values.

Pulsed eddy current signal has rich information in time domains. Various features could be extracted from picked up secondary magnetic field in time domain such as amplitude, time to peak, or time to zero crossings.

Figure 1 presents an excitation pulse in both time and frequency domains. The pulse has a duration of τ=1 ms and is repeated every T_0= 5 ms. The bars in Fig. 1-b are obtained using fast Fourier transform of the time domain signal and the envelop represent the analytical Fourier spectrum V(f) multiplied by sampling frequency f_S, where V(f) is given as [Carlson, 03]

$$V(f) = \frac{A}{f_p} \operatorname{sinc} \frac{f}{f_p} \qquad (1)$$

Where A is the magnitude of the pulse, and $f_p=1/\tau$.

It is apparent that most of energy is concentrated in the lower frequency band, and that there are repeated nulls in the spectrum. More insight into material characteristics could be obtained by enrichment of the spectrum information available from PEC inspection with information that might available at particular spectrum nodes obtained using harmonic eddy current inspection.

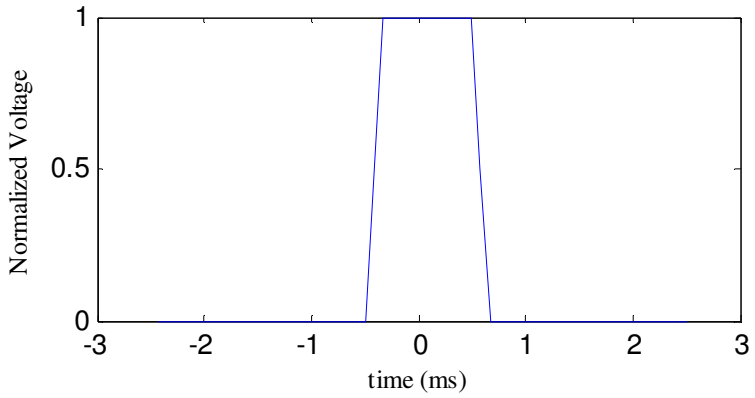

(a)

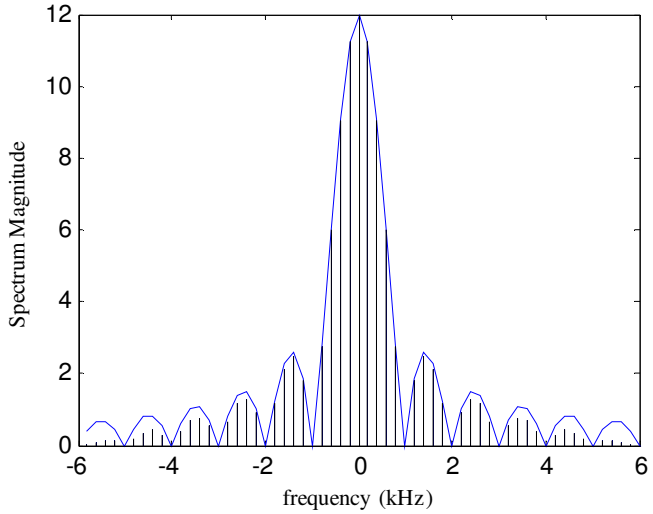

(b)

Fig. 1. Typical PEC excitation pulse in time domain (a) and spectrum of frequency domain (b).

3. EDDY CURRENT IMAGE FUSION

The concept of image fusion is done naturally by the human eye in fusing spectral color information to enhance perception of objects. Similar concept can be adopted in fusion of eddy current images. C-scan images acquired either using PEC inspection with different time domain parameters, or harmonic eddy current at various frequencies can be fused to obtain one color image. A simple algorithm is to consider three of theses images to be the RGB planes of a false color image. The resulting image that is augmented in spectral information could further be enhanced by fusion with a high spatial resolution image that

could be acquired at high frequency eddy current testing or even with a different NDE modality such as radiography or ultrasonic imaging. This simple three-image fusion technique could not be adequate with real industrial eddy current images. Advanced fusion approaches are presented next.

4. IHS TRANSFORM FUSION

Each of the three planes of image *E* defined as (*ER*, *EG*, *EB)* Three frequency eddy current images are acquired either with PEC or harmonic EC inspection. High spatial resolution image *T* is also acquired which is generally larger in dimension than other three images. Image *T* could in general be obtained with acquisition modality that is different form eddy current. The fusion is done in the following four steps:

1. Images are co-registered.
2. For each pixel *p* in the image, the *IHS* transformation is done as in [Gonzalez-Audicana 06]. This transform, thus, leads to three images: *I*, *H*, and *S*.
3. The histogram of *T* is matched to that of obtained image *I* to obtain new image *T′*. This accounts for differences related to acquisition techniques.
4. Image *T′* is down-sampled to the size of *I,* to obtain image *T″*.
5. Image *I* is replaced with *T″*.
6. Inverse IHS transform of *(T″, H, S)* is performed to obtain fused image *E′* ≡ *(ER′, EG′, EB′)*.

5. SHIFT INVARIANT WAVELET DECOMPOSITION

A problem associated with the above method is the distortion in the spectral information, which is obtained on the expense of enhancing the spatial resolution. One solution is to apply the shift invariant wavelet transform to obtain multiresolution decomposition of image *T″*. Multiresolution wavelet analysis permits the introduction of

details between successive levels of scale or resolution. The wavelet transform decomposes the original image into a number of new images with different degrees of resolution. In opposition to the spectral information provided by Fourier transform, Wavelet analysis provides both spectral as well as spatial information [Nunez, 99]. The wavelet transform of a distribution $s(x_1,x_2)$ can be written as [Misiti, 07]

$$C(a1,b1)=\int_R\int_R s(x_1,x_2)\frac{1}{\sqrt{a_1a_2}}\psi\left(\frac{x_1-b_1}{a_1},\frac{x_2-b_2}{a_2}\right)dx_1dx_2 \qquad (2)$$

$$x=(x_1,x_2)\in R^2, a_1\in R^+-\{0\}, a_2\in R^+-\{0\}, b_1\in R, b_2\in R$$

Where a_1 and a_2 are scale parameters while b_1, and b2 are translational parameters. . The base function $\psi\left(\frac{x_1-b_1}{a_1},\frac{x_2-b_2}{a_2}\right)$ is the scaled and translated version of Mother Wavelet ψ.

The shift invariant wavelet transform that could be obtained using á trous (with holes) algorithm overcomes image artifacts [Wang, 05] and [Fowler, 05]. In this algorithm, images I and T'' are decomposed as follows [Pradhan, 06]

$$I=a_L^I+\sum_{l=1}^{L}h_l^I+\sum_{l=1}^{L}v_l^I+\sum_{l=1}^{L}d_l^I \qquad (3)$$

$$T''=a_L^T+\sum_{l=1}^{L}h_l^T+\sum_{l=1}^{L}v_l^T+\sum_{l=1}^{L}d_l^T \qquad (4)$$

Where L represents the number of decomposition levels, and a^I and a^T represent the approximation matrices of I and T'' matrices respectively. The h_l, v_l, and d_l matrices are the detail images decomposition at successively higher scale.

The approximation image a_L^I is added to the detail images of the T'' image. The inverse wavelet transform is then obtained to obtain fused intensity image I_w such that

$$I_w=a_L^I+\sum_{l=1}^{L}h_l^T+\sum_{l=1}^{L}v_l^T+\sum_{l=1}^{L}d_l^T \qquad (5)$$

The inverse IHS transform is then applied to (I_w, H, S) to obtain the fused image $E' \equiv (ER', EG', EB')$. The validity of the fused image should be tested with quality metrics as described next.

6. IMAGE QUALITY METRICS

Two quality metrics are implemented based on spectral as well as spatial quality assessments 0[Wang, 05] and [Choi, 06]. The first image quality metric *IQM1* is based on the spectral analysis and is taken as the average of the three correlation coefficients such that

$$IQM1 = C(E_i \mid E_i') \tag{6}$$

with i=1, 2, and 3 for the three color planes in E and E' images. The second image quality metric *IMQ2* depends on spatial quality assessment based on structural similarity (SS) measurement, introduced in [Wang, 04]. The metric is taken to be

$$IQM2 = SS(T'' \mid E_i') \tag{7}$$

The presented fusion algorithms have been tested using simulated results obtained with finite element modeling described next.

7. COMPUTATIONAL MODELING

The differential equations for magnetic vector potential can be written as

$$\nabla \times \nu(\nabla \times \boldsymbol{A}) - \nabla \nu(\nabla \cdot \boldsymbol{A}) + \sigma \frac{\partial \boldsymbol{A}}{\partial t} + \sigma \nabla V = 0 \tag{8}$$

$$\nabla \cdot \left(\sigma \frac{\partial \boldsymbol{A}}{\partial t} + \sigma \nabla V \right) = 0 \tag{9}$$

Where $\boldsymbol{A}$ is the magnetic vector potential and V is the electric scalar potential, and σ is the conductivity. The reluctivity ν is the inverse of permeability.

For source regions, Equation 7 becomes

$$\nabla \times \nu(\nabla \times \boldsymbol{A}) - \nabla \nu(\nabla \cdot \boldsymbol{A}) = \boldsymbol{J}_s \tag{10}$$

Where, $\boldsymbol{J}_s$ is the current density in the source. The potential functions can be found by solving equations (7-9), with the appropriate boundary conditions. The finite element (FE) method is one of the best well known numerical methods that can be used to solve this problem. The FE does not offer a solution to the diffusion equation directly. Instead, the solution is obtained at discrete nodes in the solution region by formulating an energy functional equivalent to energy balance of Equations 8-10.

A three dimensional model is built to simulate a coil on top of a metal object with defects as shown in Fig. 2. The coil is designed to be of 10-mm outer radius, 5-mm inner radius, and 5-mm height. The object is composed of aluminum with 100-mm radius and 10mm thickness, and the lift-off between the probe and the object is of 1.1-mm.

Analysis is done under ANSYS environment, using electromagnetic-circuit field coupling analysis. The stranded coil is modeled to be excited from a voltage source. The element matrix is represented as [Ansys]

$$\begin{bmatrix} [0] & [0] \\ [C_{iA}] & [0] \end{bmatrix} \begin{bmatrix} \dfrac{\partial \mathbf{A}}{\partial t} \\ \mathbf{0} \end{bmatrix} + \begin{bmatrix} [K_{AA}] & [K_{Ai}] \\ [0] & [K_{ii}] \end{bmatrix} \begin{bmatrix} \mathbf{A} \\ \mathbf{0} \end{bmatrix} = \begin{bmatrix} \mathbf{0} \\ \mathbf{V_0} \end{bmatrix} \tag{11}$$

Where **A** is nodal magnetic potential vector, and **i** nodal electric current vector. K_{AA} is the potential stiffness matrix, K_{ii} resistive stiffness matrix, K_{Ai} is potential-current coupling stiffness matrix, and C_{iA} is inductive damping matrix. The vector $\mathbf{V_0}$ represents the applied voltage drop.

Three cracks are modeled in the simulation. All cracks have the same cross section of 2mm×2mm that is parallel to the object upper surface. Type I is a surface crack of 5

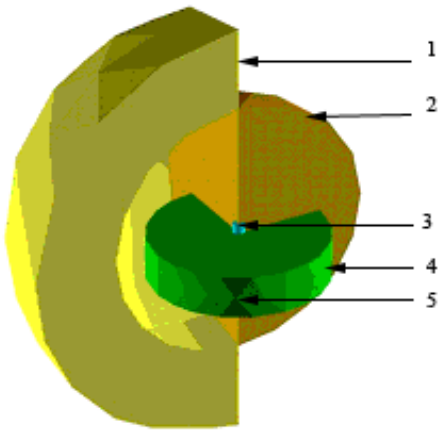

Fig. 2. Schematic finite element model of the numerical eddy current inspection system.

mm depth. Type II crack is a subsurface crack of 3mm depth and is present 1 mm under the upper surface of the object. Type III crack is of 1 mm depth and is present at 3 mm from the top surface.

A number of 117385 mesh elements are generated for acceptable accuracy. The excitation is applied and the model is solved for various crack positions and also corresponding to various excitation frequencies. Infinite boundary elements are implemented to model the surrounding infinite space.

Two formulation cases are considered as follows:

A. Analysis for sinusoidal eddy current excitation is obtained using FE harmonic analysis.

B. Pulsed eddy current is analyzed either using transient time domain analysis or a series of harmonic analysis.

In the transient analysis, a sufficiently small time step is used and time difference approach is used in time. In the harmonic analysis of PEC technique the FE model is run to obtain magnetic flux density $\boldsymbol{B}_{FE}(f)$ corresponding to frequencies kf_0, where f_0 is the inverse of repetition period T_0 and k=1, 2, ...N/2, and N is the total number of time or

frequency samples. Runs are excluded for frequencies *mfp* where f_P is the inverse of pulse period τ and m is an integer. The spectrum of magnetic flux density is obtained as

$$B(f) = V(f) B_{FE}(f) \tag{12}$$

Negative frequencies results are obtained as the conjugate of the simulation results corresponding positive frequency. Inverse Fourier transform of *B(f)* is invoked to obtain the time domain signal.

Sequence values of probe inductance and resistance values are recorded and arranged to obtain c-scan images, which simulates an object with the three crack types described earlier. Crack 1 is on the right, crack 2 is on the left and type 3 crack is in the middle. Thirteen images generated with 128x128 resolution. Three PEC images are generated as well as ten harmonic analysis images, representing probe resistance values (5 images), probe inductance values (5 images) corresponding to frequencies of 100 Hz, 1kHz, 10 kHz, 100 kHz, and 1M Hz.

Fig. 3 presents fused images correspond to simple RGB fusion technique, identifying three cracks at different depths. Fig. 4 is based on IHS fusion with high-resolution image generated at 256x256. The estimated image quality metrics of the image in Fig. 4 were calculated to be IQM1= 0.4233 and IQM2=0.9977. Examples of image fusion with shift invariant wavelet decomposition are presented in Fig. 5, and Fig. 6, where *Daubechies* wavelets of order 6 are used. The quality metrics were calculated for image in Fig. 5 to be IQM1= 0.3754 and IQM2=0.9965. Fig. 7 presents the approximation and detail images corresponding to image *I*, where the detail coefficients of *I* are replaced with those of image *T″* shown in Fig. 8.

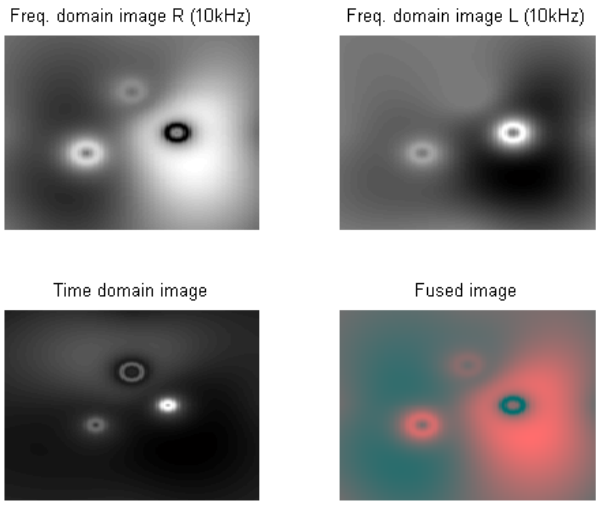

Fig. 3. Simple fusion, with 2 frequency domain images and one time domain image.

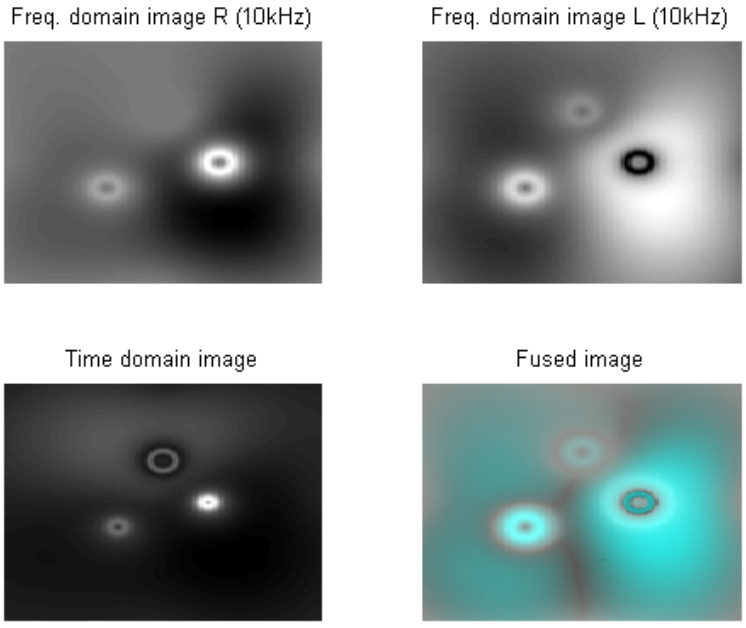

Fig. 4. Fusion obtained with IHS transformation.

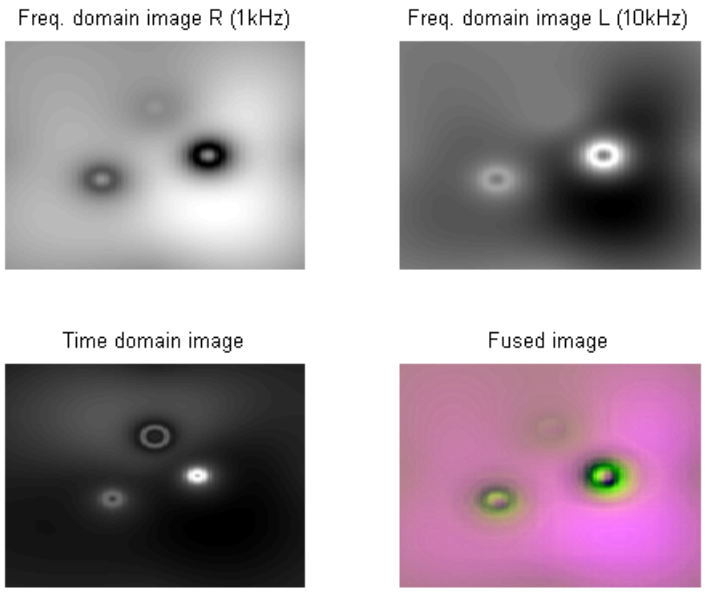

Fig. 5. Fusion obtained with wavelet decomposition, where the high spatial resolution image *T* is frequency domain image.

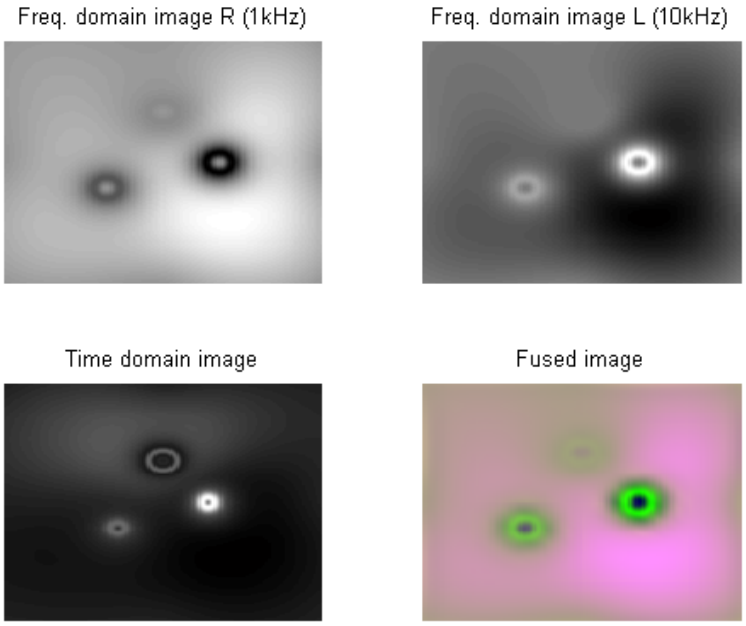

Fig. 6. Fusion obtained with wavelet decomposition as described, where the high spatial resolution image *T* is time domain image.

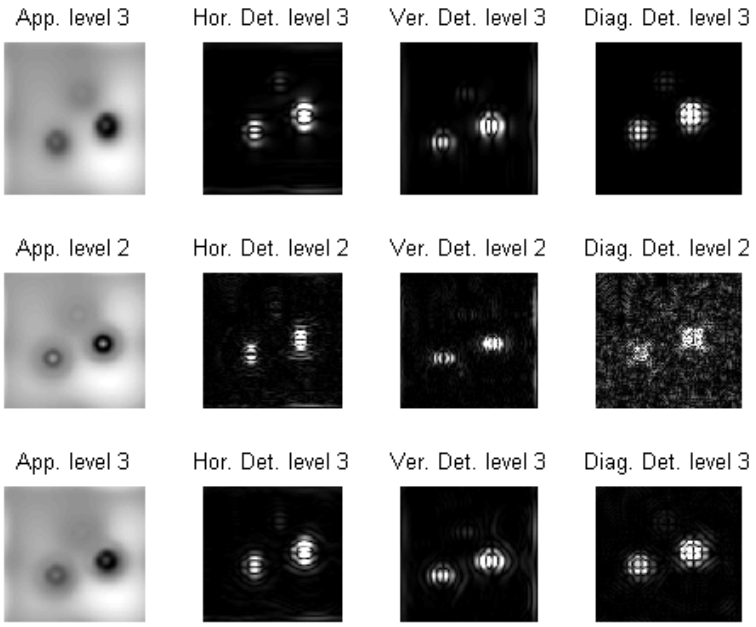

Fig. 7. Approximation and detail coefficients of image *I*. Daubechies wavelets are used.

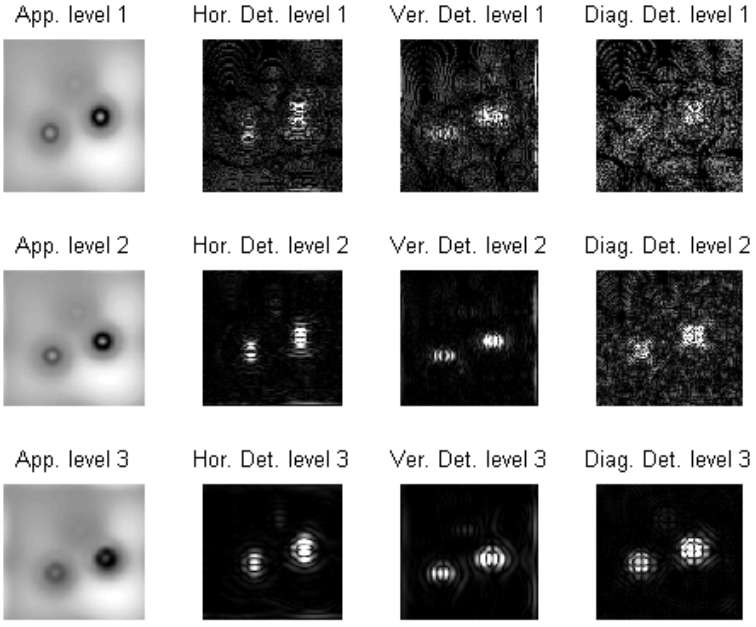

Fig. 8. Approximation and detail coefficients of image *T''*. Daubechies wavelets are used.

8. CONCLUSIONS

Enhancement of eddy current inspection in nondestructive evaluation applications is currently directed into increasing sensitivity to subsurface flaws, while maintaining high spatial resolution. Conventional eddy current using single-frequency excitation has limited material characterization capabilities and data that are more rigorous could be obtained by augmenting the spectral information with techniques such as multifrequency or swept frequency inspection. Broadband excitation is also implemented with time-domain inspection using pulsed eddy current PEC. PEC spectrum has repeated nulls and the energy decays with increase of frequency.

An algorithm, termed transfusion is presented based on fusing partial eddy current information obtained from PEC inspection with frequency nodes in the spectrum obtained by harmonic inspection. The technique is based on image fusion methods, in accordance with increased interest in C-scan representation of eddy current signals. Multi-spectral and multi-temporal data are packed into the color components of transfusion image. Further enhancement could be obtained by fusing this image with a high quality image of the object under test, which could be acquired using high frequency eddy current inspection or another NDE modality. Results based on the proposed technique, implementing finite element simulation of eddy current inspection are presented, along with suggested image quality measures to test the spectral as well as spatial information of the transfusion image.

ACKNOWLEDGMENTS

This research is funded by *King Abdulaziz City for Science and Technology* (KACST), Research Grant: 122-28.

REFERENCES

[Ansys] ANSYS documentations. www.ansys.com.

[Carlso, 03] A.B. Carlson, et al., Communication Systems: An Introduction to Signals and Noise in Electrical Communication, 4th Ed., McGraw Hill, Boston, 2002.

[Choi, 06] M. Choi, "A New Intensity-Hue-Saturation Fusion Approach to Image Fusion with a Tradeoff Parameter," *IEEE Transactions on Geoscience and Remote Sensing,* Vol. 44 (2006), pages 1672-1682.

[Fowler, 05] J. E. Fowler, "The Redundant Discrete Wavelet Transform and Additive Noise" *IEEE Signal Processing Letters*, Vol. 12 (2005), pages 629-632.

[Giguere1, 02] J.S.R. Giguere1, et al., "Detection of Cracks Beneath Rivet Heads via Pulsed Eddy Current Technique", Review of Progress in Quantitative Nondestructive Evaluation, D.O. Thompson and D.E. Chimenti, eds., Melville, New York, AIP, Vol. 21A, (2002), pages 1968-1975.

[Gonzalez-Audicana 06] M. Gonzalez-Audicana, et al., "A Low Computational-Cost Method to Fuse IKONOS Images Using the Spectral Response Function of Its Sensors," *IEEE Transactions on Geoscience and Remote Sensing,* Vol. 44 (2006), pages 1683-1691.

[Misiti, 07] M. Misiti, et al., Matlab Wavelet Toolbox 4, User's Guide, www.mathworks.com.

[Nunez, 99] J. Nunez et al., "Multiresolution-Based Image Fusion with Additive Wavelet Decomposition, IEEE *Transactions on Geoscience and Remote Sensing,* Vol. 37 (1999) pages 1204-1211.

[Plotnikiv, 02] Y.A. Plotnikov, et al., "Defect Characterization in Multi-Layered Conductive Components with Pulsed Eddy Current," Review of Progress in Quantitiative Nondestructive Evaluation, D.O. Thompson and D.E. Chimenti, eds., Melville, New York, AIP, Vol. 21A, (2002), pages 1976-1983.

[Plotnikov, 07] Y.A. Plotnikov, et al., "Enhanced Corrosion Detection in Airframe Structures Using Pulsed Eddy Current and Advanced Processing," Materials Evaluation, April 2007, pages 403-410.

[Pradhan, 06] P. S. Pradhan, et al., "Estimation of the Number of Decomposition Levels for a Wavelet-Based Multiresolution Multisensor Image Fusion," *IEEE Transactions on Geoscience and Remote Sensing*, Vol. 44 (2006), pages 3674-3686.

[Udpa, 01] L. Udpa, and I. Elshafiey, "WINSADS: A New tool for Enhancing the Performance of Eddy Current Inspection of Aging Aircraft Wheels," Invited Paper, *Proceeding of The 5th Joint NASA/FAA/DoD Conference on Aging Aircraft*, Hyatt-Orlando, Orlando, Florida September, 2001.

[Wang, 04] Z. Wang, et al., "Image Quality Assessment: From Error Visibility to Structural Similarity," *IEEE Transactions on Image Processing*, Vol. 13 (2004), pages 600-612.

[Wang, 05] Z. Wang, et al., "A Comparative Analysis of Image Fusion Methods," *IEEE Transactions on Geoscience and Remote Sensing,* Vol. 43 (2005), pages 1391-1402.